Supporting Information for

Peroxido-bridged chiral double-decker dysprosium macrocycles

Chen Zhao,[a,b,‡] Tingting Wang,[a,b,‡] Xiaodong Liu,[a,b] Zhenhua Zhu,*[a,c] Xu Ying,[a,b] Xiao-Lei Li[a] and Jinkui Tang*[a,b]

[a]State Key Laboratory of Rare Earth Resource Utilization, Changchun Institute of Applied Chemistry, Chinese Academy of Sciences, Changchun, 130022, P. R. China
[b]School of Applied Chemistry and Engineering, University of Science and Technology of China, Hefei, 230026, P. R. China
[c]University of Chinese Academy of Sciences, Beijing, 100049, P. R. China
[‡]These authors contributed equally to this work.
*Corresponding authors. Email: zhuzh@ciac.ac.cn; tang@ciac.ac.cn

Contents

X-ray crystallography

Table S1. Crystal Data and Structure Refinement for **1** and **2**.

Compound reference	1	2
Chemical formula	$C_{183}H_{159}B_2Dy_2N_{19}O_5$	$C_{180}H_{154.5}B_2Dy_2N_{17.5}O_5$
Formula Mass	3050.90	2989.32
Temperature (K)	180.0	180.0
Crystal system	monoclinic	monoclinic
Space group	$C2$	$C2$
a (Å)	29.7238(10)	29.7543(12)
b (Å)	17.4037(6)	17.3502(7)
c (Å)	62.791(2)	62.722(2)
α (°)	90	90
β (°)	103.2170(10)	103.1690(10)
γ (°)	90	90
Unit cell volume (Å³)	31621.5(19)	31528(2)
Z	8	8
ρ_{calc} (g/cm³)	1.282	1.260
μ / mm^{-1}	1.001	1.002
F (000)	12576.0	12312
Radiation	MoKα (λ = 0.71073)	MoKα (λ = 0.71073)
Reflections collected	160554	131144
Independent reflections	55747	54639
R_{int}	0.0496	0.1338
GOF on F^2	1.028	1.001
R_1 ($I \geq 2\sigma$ (I))	0.0400	0.1029
wR_2 (all data)	0.0843	0.3448
CCDC number	2223655	2223656

Table S2. Selected bond distances (Å) for complexes **1** and **2**.

	1		2
Dy1–O1	2.160(5)	Dy1–O1	2.232(17)
Dy1–O2	2.238(6)	Dy1–O2	2.202(18)
Dy1–O3	2.242(5)	Dy1–O3	2.207(16)
Dy2–O2	2.255(5)	Dy2–O2	2.299(17)
Dy2–O3	2.254(5)	Dy2–O3	2.247(17)
Dy2–O4	2.194(5)	Dy2–O4	2.138(18)
Dy3–O5	2.189(4)	Dy3–O5	2.187(16)
Dy3–O6	2.243(5)	Dy3–O6	2.281(16)
Dy3–O7	2.248(5)	Dy3–O7	2.249(16)
Dy4–O6	2.254(5)	Dy4–O6	2.209(16)
Dy4–O7	2.233(5)	Dy4–O7	2.231(17)
Dy4–O8	2.175(4)	Dy4–O8	2.205(16)
Dy1–N1	2.685(6)	Dy1–N1	2.70(2)
Dy1–N2	2.648(6)	Dy1–N2	2.69(2)
Dy1–N3	2.701(6)	Dy1–N3	2.71(2)
Dy1–N4	2.696(6)	Dy1–N4	2.62(2)
Dy1–N5	2.655(5)	Dy1–N5	2.71(2)
Dy1–N6	2.688(6)	Dy1–N6	2.65(2)
Dy2–N7	2.606(6)	Dy2–N7	2.64(2)
Dy2–N8	2.681(5)	Dy2–N8	2.69(2)
Dy2–N9	2.650(6)	Dy2–N9	2.61(2)
Dy2–N10	2.588(6)	Dy2–N10	2.60(2)
Dy2–N11	2.668(6)	Dy2–N11	2.67(2)
Dy2–N12	2.616(5)	Dy2–N12	2.62(2)
Dy3–N13	2.611(5)	Dy3–N13	2.58(2)
Dy3–N14	2.613(6)	Dy3–N14	2.63(2)
Dy3–N15	2.715(6)	Dy3–N15	2.71(2)
Dy3–N16	2.662(6)	Dy3–N16	2.66(2)
Dy3–N17	2.603(6)	Dy3–N17	2.59(2)
Dy3–N18	2.658(5)	Dy3–N18	2.60(2)
Dy4–N19	2.681(6)	Dy4–N19	2.70(2)
Dy4–N20	2.699(6)	Dy4–N20	2.67(2)
Dy4–N21	2.679(6)	Dy4–N21	2.63(2)
Dy4–N22	2.678(6)	Dy4–N22	2.69(2)
Dy4–N23	2.681(6)	Dy4–N23	2.62(2)
Dy4–N24	2.641(6)	Dy4–N24	2.60(2)
O2–O3	1.495(6)	O2–O3	1.46(2)
O6–O7	1.494(6)	O6–O7	1.48(2)

Table S3. Selected bond angles (°) for complexes **1** and **2**.

1		2	
Dy1–O2–Dy2	141.3(2)	Dy1–O2–Dy2	140.1(8)
Dy1–O3–Dy2	141.0(2)	Dy1–O3–Dy2	143.6(9)
Dy3–O6–Dy4	140.5(2)	Dy3–O6–Dy4	141.0(8)
Dy3–O7–Dy4	141.7(2)	Dy3–O7–Dy4	141.7(8)
O1–Dy1–O2	161.09(18)	O1–Dy1–O2	160.6(6)
O1–Dy1–O3	159.45(18)	O1–Dy1–O3	160.6(7)
O4–Dy2–O2	162.47(18)	O4–Dy2–O2	162.5(7)
O4–Dy2–O3	158.79(18)	O4–Dy2–O3	160.0(6)
O5–Dy3–O6	158.34(17)	O5–Dy3–O6	158.4(6)
O5–Dy3–O7	162.89(17)	O5–Dy3–O7	163.2(6)
O8–Dy4–O6	160.89(18)	O8–Dy4–O6	160.1(6)
O8–Dy4–O7	159.82(17)	O8–Dy4–O7	159.6(6)
N1–Dy1–N2	60.15(18)	N1–Dy1–N2	60.2(7)
N2–Dy1–N3	60.40(18)	N2–Dy1–N3	57.5(7)
N3–Dy1–N4	60.20(17)	N3–Dy1–N4	62.0(7)
N4–Dy1–N5	60.46(17)	N4–Dy1–N5	61.6(7)
N5–Dy1–N6	60.42(18)	N5–Dy1–N6	59.4(7)
N6–Dy1–N1	60.58(18)	N6–Dy1–N1	61.6(7)
N7–Dy2–N8	60.42(17)	N7–Dy2–N8	60.7(7)
N8–Dy2–N9	60.65(18)	N8–Dy2–N9	59.5(7)
N9–Dy2–N10	60.54(18)	N9–Dy2–N10	61.2(7)
N10–Dy2–N11	60.94(18)	N10–Dy2–N11	60.6(7)
N11–Dy2–N12	60.71(18)	N11–Dy2–N12	60.9(7)
N12–Dy2–N7	61.53(18)	N12–Dy2–N7	62.2(7)
N13–Dy3–N14	61.37(18)	N13–Dy3–N14	61.3(7)
N14–Dy3–N15	60.50(18)	N14–Dy3–N15	58.3(7)
N15–Dy3–N16	59.33(17)	N15–Dy3–N16	60.9(7)
N16–Dy3–N17	61.32(17)	N16–Dy3–N17	62.0(6)
N17–Dy3–N18	60.77(18)	N17–Dy3–N18	61.6(7)
N18–Dy3–N13	61.26(17)	N18–Dy3–N13	60.3(7)
N19–Dy4–N20	60.33(19)	N19–Dy4–N20	61.8(7)
N20–Dy4–N21	60.07(18)	N20–Dy4–N21	58.9(7)
N21–Dy4–N22	60.19(18)	N21–Dy4–N22	60.3(6)
N22–Dy4–N23	60.81(18)	N22–Dy4–N23	62.0(7)
N23–Dy4–N24	60.71(17)	N23–Dy4–N24	61.0(7)
N24–Dy4–N19	60.13(18)	N24–Dy4–N19	58.3(7)

Table S4. Crystal Data and Structure Refinement for **3** and **4**

Compound reference	3	4
Chemical formula	$C_{144}H_{126}B_2Cl_2Dy_2N_{18}O_2$	$C_{144}H_{126}B_2Cl_2Dy_2N_{18}O_2$
Formula Mass	2558.14	2558.14
Temperature (K)	180.0	180.0
Crystal system	orthorhombic	orthorhombic
Space group	$P2_12_12_1$	$P2_12_12_1$
a (Å)	15.7298(3)	15.7450(3)
b (Å)	16.3326(4)	16.3240(4)
c (Å)	47.7251(10)	47.7781(12)
α (°)	90	90
β (°)	90	90
γ (°)	90	90
Unit cell volume (Å^3)	12261.0(5)	12280.0(5)
Z	4	4
ρ_{calc} (g/cm^3)	1.386	1.384
μ / mm^{-1}	1.315	1.313
F (000)	5232.0	5232.0
Radiation	MoKα (λ = 0.71073)	MoKα (λ = 0.71073)
Reflections collected	90517	83424
Independent reflections	21667	21647
R_{int}	0.0681	0.0503
GOF on F^2	1.061	1.032
R_1 ($I \geq 2\sigma$ (I))	0.0474	0.0438
wR_2 (all data)	0.1321	0.1149
CCDC number	2228952	2228983

Table S5. Selected bond distances (Å) for complexes **3** and **4**.

	3		**4**	
Dy1–Cl1	2.663(3)	Dy1–Cl1	2.639(2)
Dy2–Cl2	2.640(3)	Dy2–Cl2	2.669(3)
Dy1–O1	2.274(6)	Dy1–O1	2.265(5)
Dy1–O2	2.236(7)	Dy1–O2	2.263(6)
Dy2–O1	2.255(6)	Dy2–O1	2.258(5)
Dy2–O2	2.255(7)	Dy2–O2	2.237(6)
Dy1–N1	2.648(7)	Dy1–N1	2.635(7)
Dy1–N2	2.664(9)	Dy1–N2	2.639(6)
Dy1–N3	2.640(9)	Dy1–N3	2.629(7)
Dy1–N4	2.621(8)	Dy1–N4	2.627(6)
Dy1–N5	2.633(8)	Dy1–N5	2.680(7)
Dy1–N6	2.620(8)	Dy1–N6	2.644(7)
Dy2–N7	2.621(7)	Dy2–N7	2.638(7)
Dy2–N8	2.637(8)	Dy2–N8	2.668(8)
Dy2–N9	2.629(7)	Dy2–N9	2.642(7)
Dy2–N10	2.648(7)	Dy2–N10	2.631(7)
Dy2–N11	2.684(8)	Dy2–N11	2.630(7)
Dy2–N12	2.624(7)	Dy2–N12	2.598(7)
O1–O2	1.546(9)	O1–O2	1.532(8)

Table S6. Selected bond angles (°) for complexes **3** and **4**.

	3		**4**	
Dy1–O1–Dy2	138.5(3)	Dy1–O1–Dy2	139.5(3)
Dy1–O2–Dy2	141.2(3)	Dy1–O2–Dy2	141.1(3)
Cl1–Dy1–O1	158.09(18)	Cl1–Dy1–O1	161.89(15)
Cl1–Dy1–O2	161.55(19)	Cl1–Dy1–O2	158.34(16)
Cl2–Dy2–O1	161.58(18)	Cl2–Dy2–O1	158.76(16)
Cl2–Dy2–O2	158.22(18)	Cl2–Dy2–O2	161.22(16)
N1–Dy1–N2	59.8(3)	N1–Dy1–N2	60.5(2)
N2–Dy1–N3	60.1(3)	N2–Dy1–N3	61.1(2)
N3–Dy1–N4	60.8(3)	N3–Dy1–N4	60.6(2)
N4–Dy1–N5	61.0(3)	N4–Dy1–N5	60.4(2)
N5–Dy1–N6	60.9(3)	N5–Dy1–N6	61.1(2)
N6–Dy1–N1	60.5(2)	N6–Dy1–N1	60.7(2)
N7–Dy2–N8	60.7(2)	N7–Dy2–N8	60.1(2)
N8–Dy2–N9	60.9(2)	N8–Dy2–N9	59.9(2)
N9–Dy2–N10	60.7(2)	N9–Dy2–N10	60.5(2)
N10–Dy2–N11	61.0(3)	N10–Dy2–N11	61.1(2)
N11–Dy2–N12	59.7(2)	N11–Dy2–N12	60.8(2)
N12–Dy2–N7	61.2(2)	N12–Dy2–N7	61.3(2)

Table S7. The CShM values calculated by SHAPE 2.1 for **1**. The lowest CShM value is highlighted.[1, 2]

Coordination Geometry	1			
	Dy1	Dy2	Dy3	Dy4
Enneagon (D_{9h})	34.610	34.479	34.793	34.124
Octagonal pyramid (C_{8v})	24.929	25.686	25.854	25.055
Heptagonal bipyramid (D_{7h})	16.177	16.711	16.482	15.788
Johnson triangular cupola J3 (C_{3v})	15.214	14.420	14.222	15.263
Capped cube J8 (C_{4v})	8.314	6.681	6.650	8.333
Spherical-relaxed capped cube (C_{4v})	7.227	5.538	5.512	7.182
Capped square antiprism J10 (C_{4v})	12.003	12.542	12.640	11.889
Spherical capped square antiprism (C_{4v})	11.855	12.423	12.473	11.825
Tricapped trigonal prism J51 (D_{3h})	11.237	11.989	12.071	11.168
Spherical tricapped trigonal prism (D_{3h})	12.286	12.763	12.803	12.309
Tridiminished icosahedron J63 (C_{3v})	9.664	11.117	11.006	9.832
Hula-hoop (C_{2v})	1.923	2.262	2.243	1.900
Muffin (C_s)	10.057	10.439	10.516	10.020

Table S8. The CShM values calculated by SHAPE 2.1 for **2**. The lowest CShM value is highlighted.[1, 2]

Coordination Geometry	2			
	Dy1	Dy2	Dy3	Dy4
Enneagon (D_{9h})	34.792	34.660	35.174	34.042
Octagonal pyramid (C_{8v})	24.587	25.496	25.595	24.869
Heptagonal bipyramid (D_{7h})	15.765	16.690	16.789	15.563
Johnson triangular cupola J3 (C_{3v})	15.070	13.965	13.941	15.227
Capped cube J8 (C_{4v})	8.233	6.819	6.920	8.019
Spherical-relaxed capped cube (C_{4v})	7.177	5.579	5.745	6.887
Capped square antiprism J10 (C_{4v})	11.726	12.915	12.637	11.709
Spherical capped square antiprism (C_{4v})	11.711	12.782	12.560	11.558
Tricapped trigonal prism J51 (D_{3h})	11.315	12.267	12.101	11.061
Spherical tricapped trigonal prism (D_{3h})	12.259	13.049	12.816	12.128
Tridiminished icosahedron J63 (C_{3v})	9.847	11.148	10.844	10.013
Hula-hoop (C_{2v})	1.977	2.477	2.220	1.965
Muffin (C_s)	9.936	10.725	10.765	9.691

Table S9. The CShM values calculated by SHAPE 2.1 for **3** and **4**. The lowest CShM value is highlighted.[1, 2]

Coordination Geometry	3		4	
	Dy1	**Dy2**	**Dy1**	**Dy2**
Enneagon (D_{9h})	35.339	35.403	35.581	35.420
Octagonal pyramid (C_{8v})	25.485	25.621	25.534	25.521
Heptagonal bipyramid (D_{7h})	16.507	16.093	16.097	16.629
Johnson triangular cupola J3 (C_{3v})	13.649	14.433	14.314	13.788
Capped cube J8 (C_{4v})	8.692	9.078	9.166	8.653
Spherical-relaxed capped cube (C_{4v})	7.157	7.536	7.598	7.118
Capped square antiprism J10 (C_{4v})	10.559	9.519	9.560	10.443
Spherical capped square antiprism (C_{4v})	10.113	9.135	9.186	10.013
Tricapped trigonal prism J51 (D_{3h})	10.520	9.735	9.814	10.474
Spherical tricapped trigonal prism (D_{3h})	10.299	9.436	9.493	10.245
Tridiminished icosahedron J63 (C_{3v})	7.481	8.793	8.698	7.547
Hula-hoop (C_{2v})	2.516	2.598	2.642	2.593
Muffin (C_s)	8.019	7.381	7.389	7.931

Table S10. Structural and magnetic parameters for dinuclear hexaazamacrocyclic SMMs.

Complex	**1**	**Dy_2–OH–Me**	**Dy_2–OH–SMe**	**Dy_2–F**
Dy–O/F$_{outer}$ (Å)	2.179	2.144	2.170	2.184
Dy–O/F$_{inner}$ (Å)	2.246	2.288	2.285	2.267
Dy–N$_{equatorial}$ (Å)	2.658	2.665	2.672	2.654
Dy–Dy$_{intramolecular}$ (Å)	4.236	3.828	3.822	3.808
U_{eff} (K)	60(3)	230(19)	141(6)	39(3)
C	1.4×10^{-2}	2.9	8.94	2.3
n	3.7	2.47	2.38	2.1
Hysteresis loop (1.9 K)	Yes	No	No	No
Ref.	This work	[3]	[4]	[5]

Note: All bond distances refer to the average values.
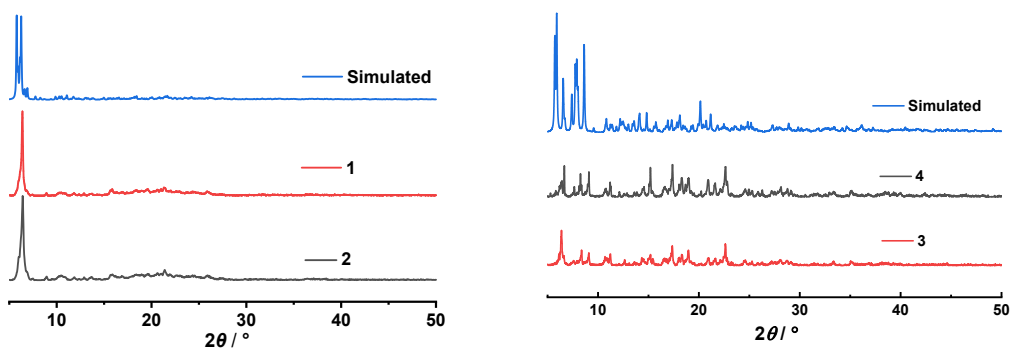
Fig. S1 Powder XRD analyses of complexes **1**-**4**. The blue lines are simulated data from single crystal data.
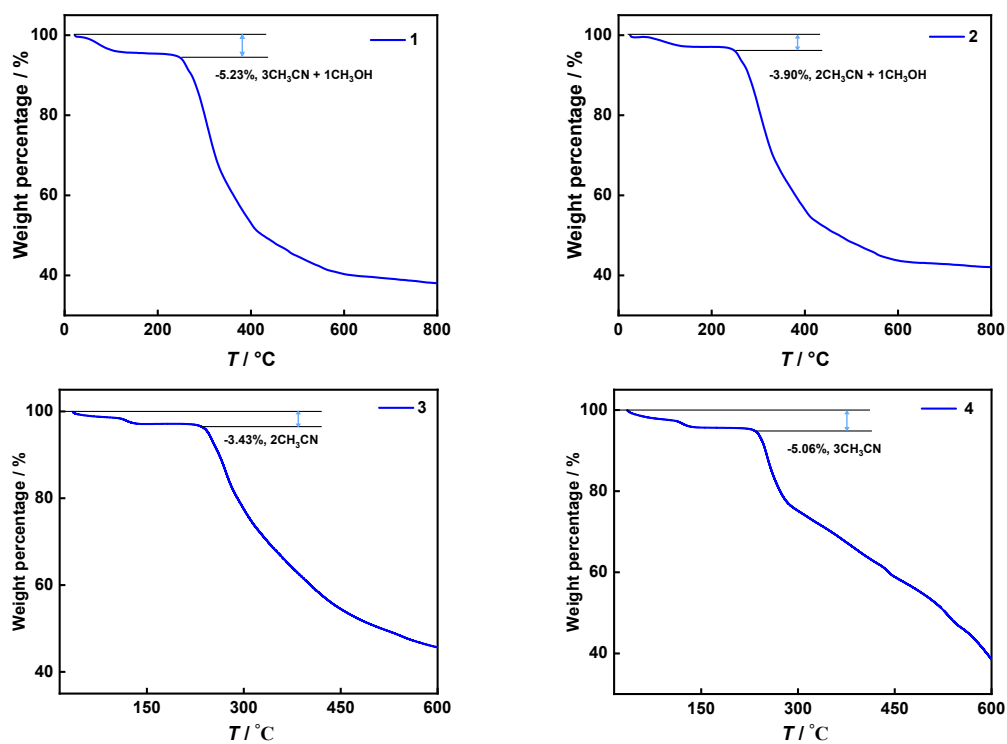
Fig. S2 Thermogravimetric analysis of complexes **1**-**4**.
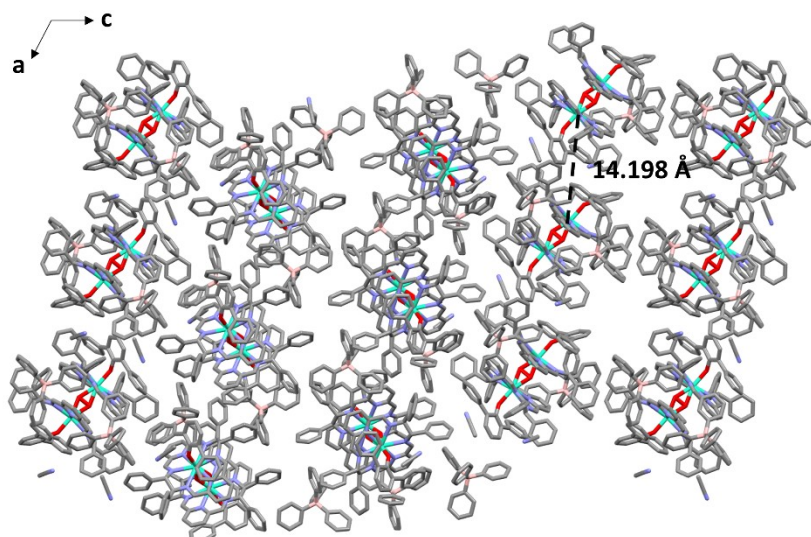
Fig. S3 The packing diagram for **1** shown along the crystallographic *b* axis gives the shortest intermolecular Dy···Dy distance of 14.198 Å. The hydrogen atoms are omitted for clarity.
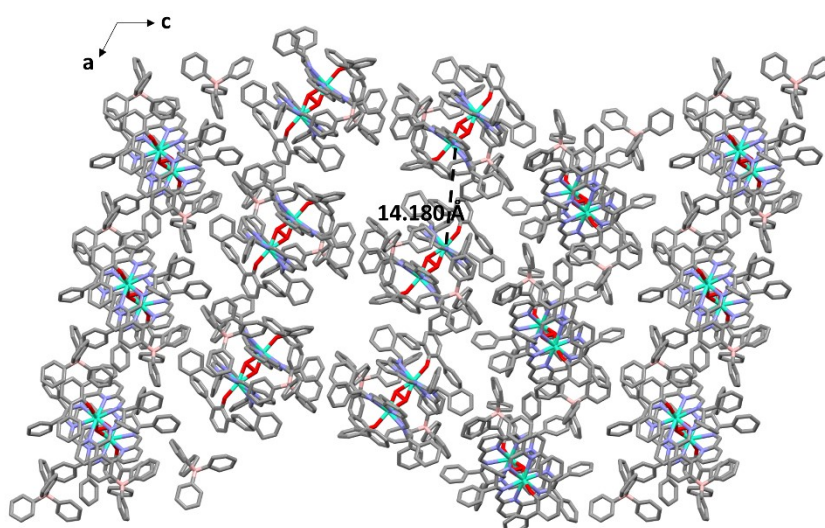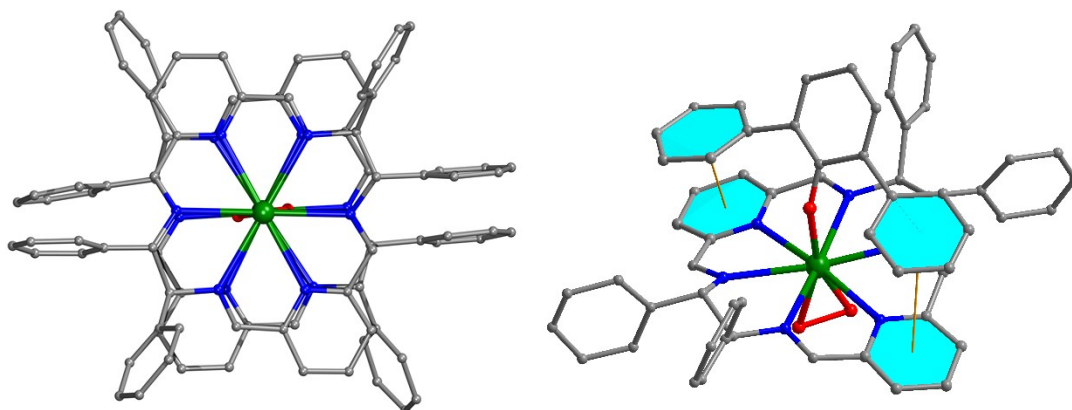

Fig. S4 The packing diagram for **2** shown along the crystallographic *b* axis gives the shortest intermolecular Dy···Dy distance of 14.180 Å. The hydrogen atoms are omitted for clarity.

Fig. S5 Crystal structure of **1** (left). Hydrogen atoms, solvents, counter ions and axial ligands are omitted for clarity. The π-π stacking interaction between the equatorial pyridine ring and one axial benzene unit in **1** (right).
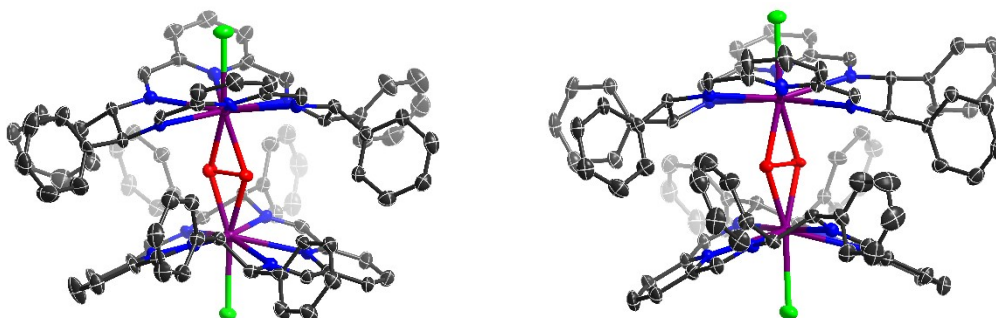
Fig. S6 Crystal structures of **3** (left) and **4** (right). Hydrogen atoms, solvents and counter ions are omitted for clarity. Displacement ellipsoids set at the 30% probability level. Color code: Dy, violet; O, red; N, blue; C, gray.
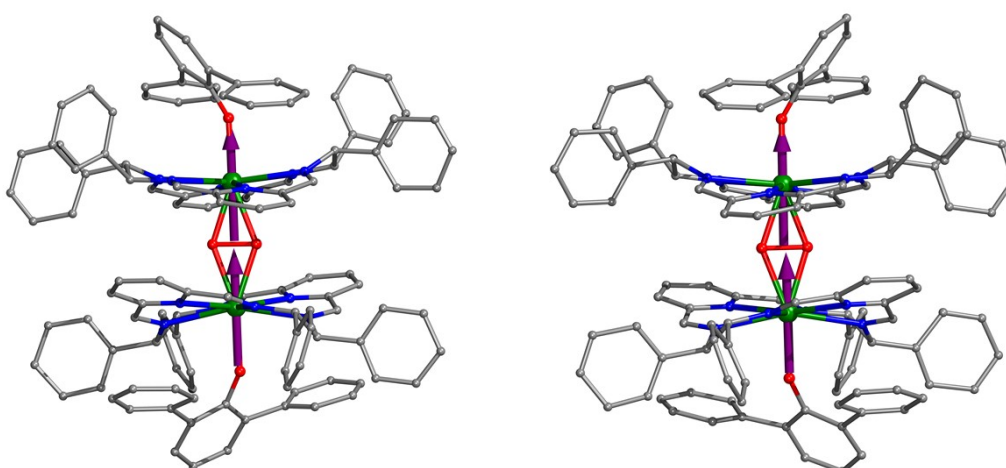
Fig S7 Ground-state magnetic anisotropy of complex **1-Dy1Dy2** (left) and **2-Dy1Dy2** (right). The violet lines represent the orientation of the anisotropy axis for Dy ions.[6]
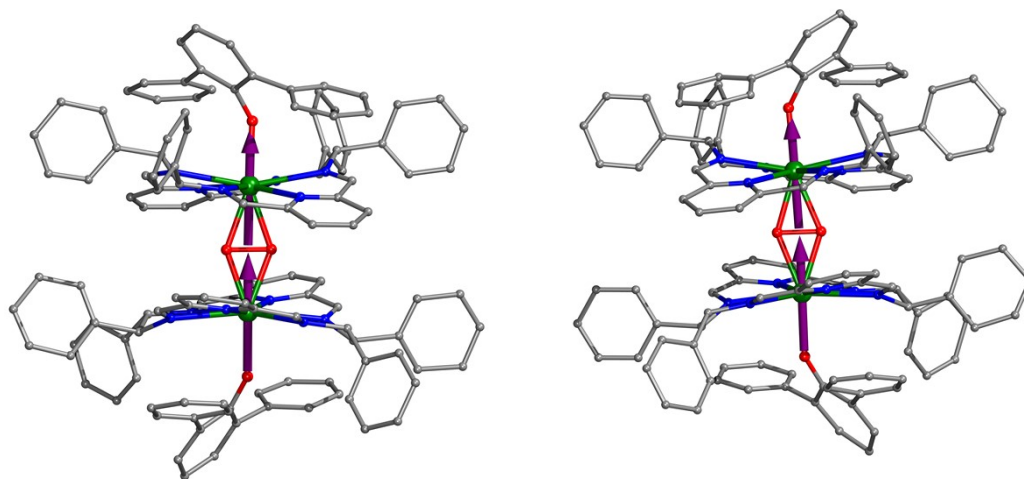
Fig S8 Ground-state magnetic anisotropy of complex **1-Dy3Dy4** (left) and **2-Dy3Dy4** (right). The violet lines represent the orientation of the anisotropy axis for Dy ions.[6]
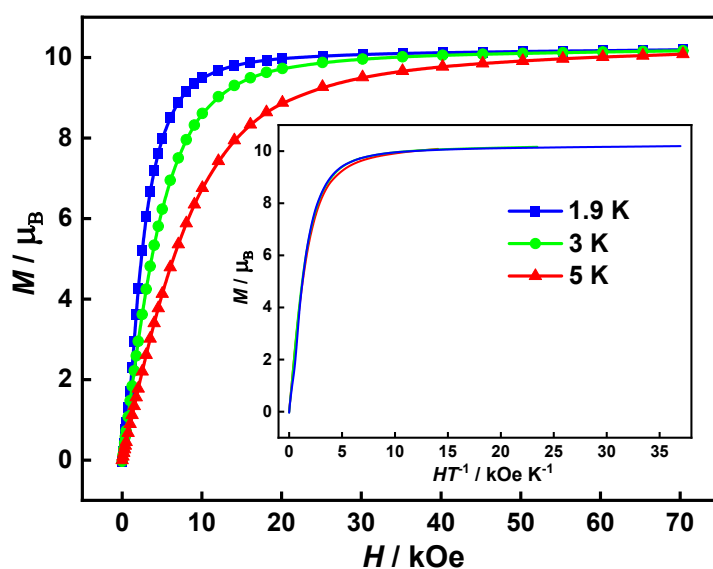
Magnetic measurements
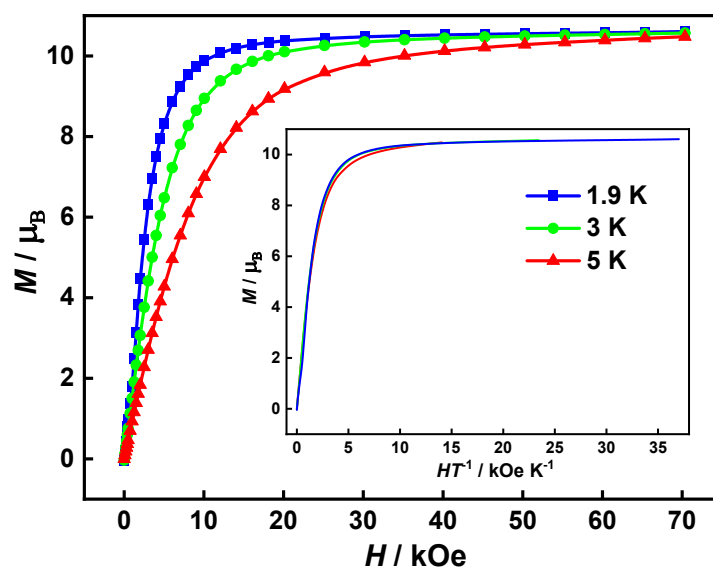
Fig. S9 Field dependence of magnetization between 0 and 70 kOe and at temperatures of 1.9, 3.0, and 5.0 K for **1**. Inset: *M vs. H/T* plots for **1** at indicated temperatures.
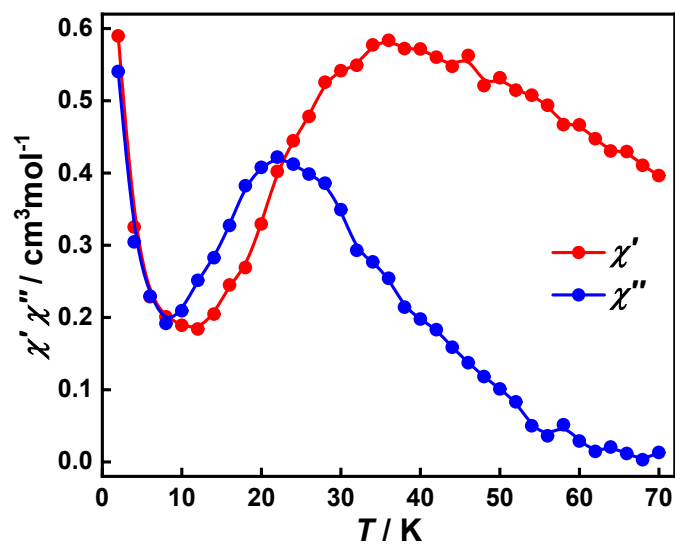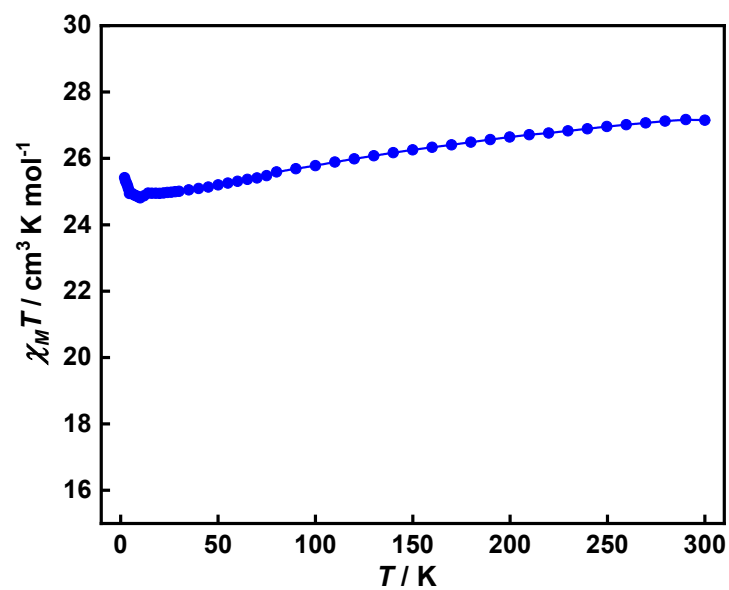
Fig. S10 Temperature dependence of in-phase (χ') and out-of-phase susceptibility (χ'') for **1** under zero dc field at 997 Hz.
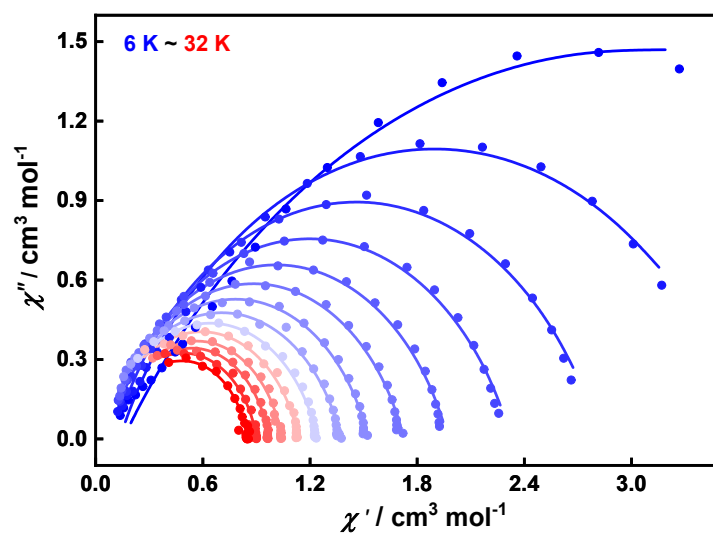
Fig. S11 Cole-Cole plots for **1**. The solid lines are obtained by fitting experimental data to generalized Debye model.
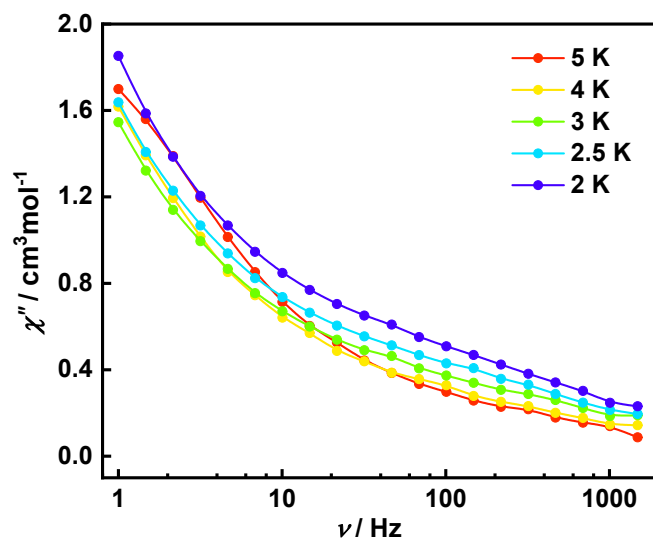
Fig. S12 Frequency dependence of the out-of-phase susceptibility (χ'') for **1** under zero dc field in the temperature range of 2-5 K. Solid lines are a guide to the eye.

Fig. S13 Field dependence of magnetization between 0 and 70 kOe and at temperatures of 1.9, 3.0, and 5.0 K for **2**. Inset: *M vs. H/T* plots for **2** at indicated temperatures.

Fig. S14 Temperature dependence of $\chi_M T$ products at 1000 Oe measured for **2**.
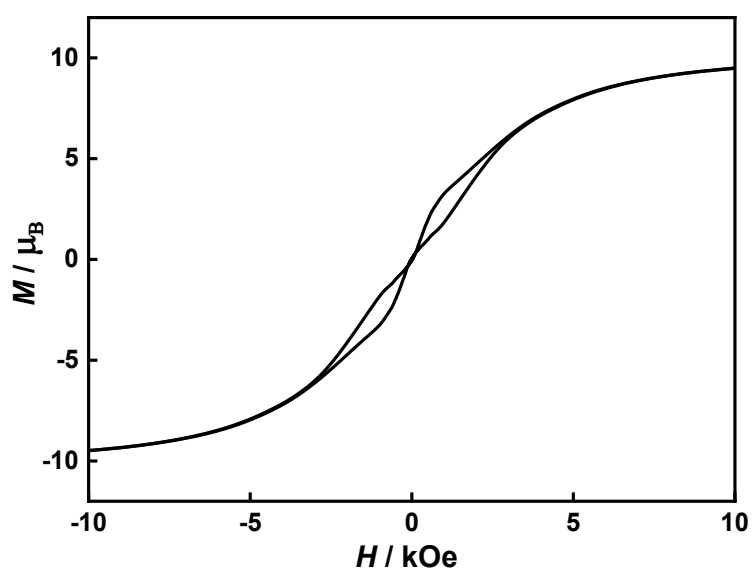
Fig. S15 Magnetic hysteresis loop for **2**. The data were collected at 1.9 K using an average field sweep speed of 18 Oe s^{-1}.
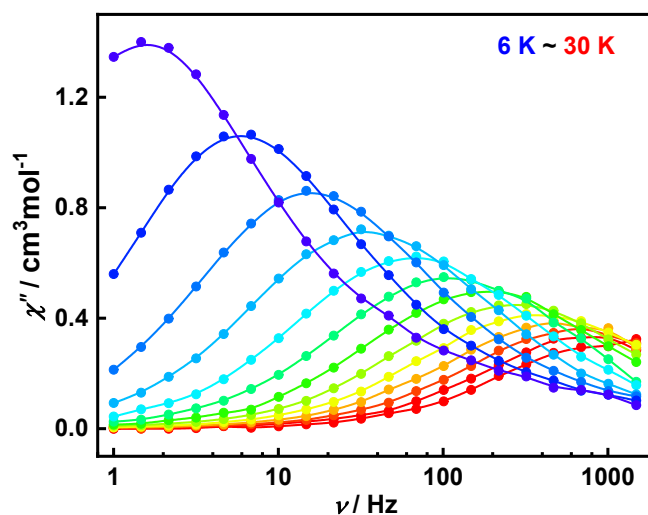
Fig. S16 Frequency dependence of the out-of-phase susceptibility (χ'') for **2** under a zero dc field at ac frequencies of 1-1488 Hz in the temperature range of 6 to 30 K (2 K interval). Solid lines are a guide to the eye.
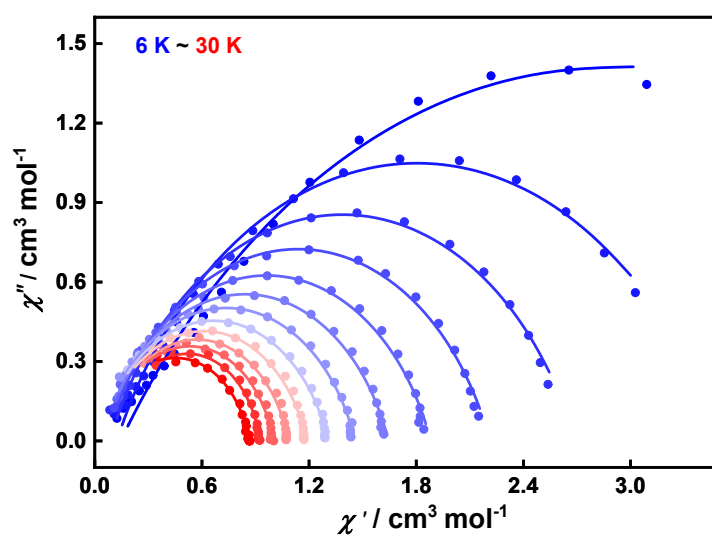

Fig. S17 Cole-Cole plots for **2**. The solid lines are obtained by fitting experimental data to generalized Debye model.
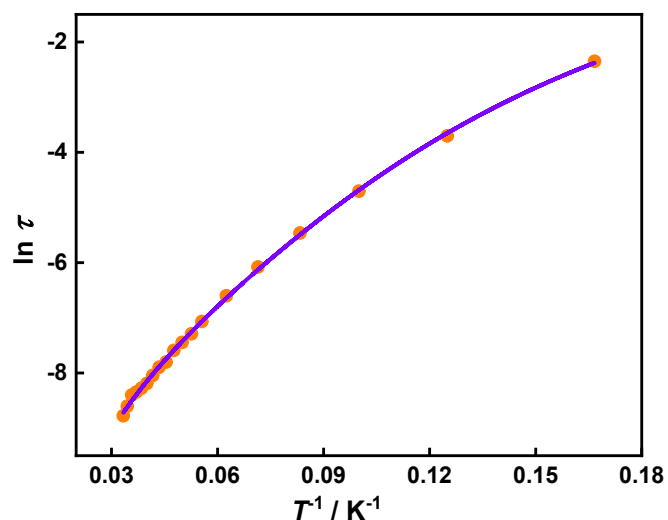
Fig. S18 Temperature dependence of the relaxation time in the form of natural logarithm for **2** under zero dc field. The solid line represents the best fit. The fitting equation is $\ln(\tau) = -\ln[CT^n + \tau_0^{-1}\exp(-U_{eff}/k_BT)]$, giving U_{eff}/k_B = 59(3) K, τ_0 = 6.4 × 10^{-5} s, C = 1.3 × 10^{-2} s^{-1}K^{-n} and n = 3.7 (adjusted R^2 = 0.9993).
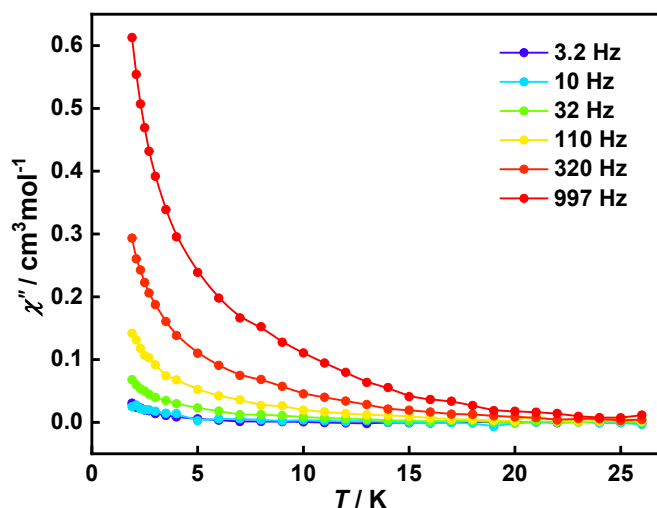

Fig. S19 Temperature dependence of out-of-phase susceptibility (χ'') for **3** under zero dc field. Solid lines are a guide to the eye.
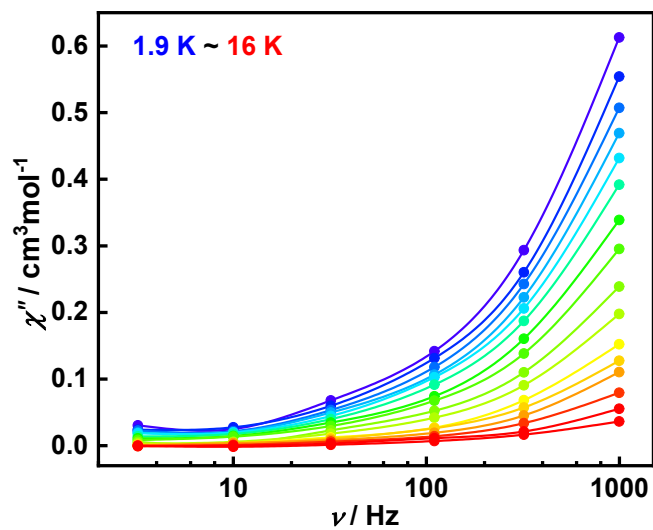
Fig. S20 Frequency dependence of out-of-phase susceptibility (χ'') for **3** under zero dc field. Solid lines are a guide to the eye.

References

1. D. Casanova, J. Cirera, M. Llunell, P. Alemany, D. Avnir and S. Alvarez, *J. Am. Chem. Soc.*, 2004, **126**, 1755-1763.
2. M. Pinsky and D. Avnir, *Inorg. Chem.*, 1998, **37**, 5575-5582.
3. C. Zhao, Z. Zhu, X.-L. Li and J. Tang, *Inorg. Chem. Front.*, 2022, **9**, 4049-4055.
4. Z. Zhu, C. Zhao, Q. Zhou, S. Liu, X.-L. Li, A. Mansikkamäki and J. Tang, *CCS Chem.*, 2022, **4**, 3762-3771.
5. X. Liu, C. Zhao, J. Wu, Z. Zhu and J. Tang, *Dalton Trans.*, 2022, **51**, 16444-16447.
6. N. F. Chilton, D. Collison, E. J. L. McInnes, R. E. P. Winpenny and A. Soncini, *Nat. Commun.*, 2013, **4**, 2551.